catalysts

MDPI

Supplementary Materials

Hydride Generation on the Cu-Doped CeO_2(111) Surface and Its Role in CO_2 Hydrogenation Reactions

Zhi-Qiang Wang [1,†], Hui-Hui Liu [1,†], Xin-Ping Wu [1,*], Peijun Hu [1,2] and Xue-Qing Gong [1,*]

[1] Key Laboratory for Advanced Materials and Joint International Research Laboratory for Precision Chemistry and Molecular Engineering, Feringa Nobel Prize Scientist Joint Research Center, Centre for Computational Chemistry and Research Institute of Industrial Catalysis, School of Chemistry and Molecular Engineering, East China University of Science and Technology, 130 Meilong Road, Shanghai 200237, China; zhiqiangwang@ecust.edu.cn (Z.-Q.W.); liuhuihui@ecust.edu.cn (H.-H.L.); p.hu@qub.ac.uk (P.H.)

[2] School of Chemistry and Chemical Engineering, The Queen's University of Belfast, Belfast BT9 5AG, UK

* Correspondence: xpwu@ecust.edu.cn (X.-P.W.); xgong@ecust.edu.cn (X.-Q.G.)

† These authors contributed equally to this work.

Table S1. Calculated lattice constants of bulk ceria by using different plane wave kinetic energy cutoffs.

kinetic Energy Cutoffs	Lattice Parameters / Å		
	a	b	c
350	5.393	5.393	5.393
400	5.456	5.456	5.456
450	5.488	5.488	5.488

Table S2. Calculated lattice constants of bulk ceria by using different *k*-point meshes.

k-point Mesh	Lattice Parameters / Å		
	a	b	c
3×3×3	5.449	5.449	5.449
5×5×5	5.456	5.456	5.456
7×7×7	5.456	5.456	5.456
9×9×9	5.456	5.456	5.456

Table S3. Calculated Bader charges of the Cu^{2+} of CuO and the Cu^{1+} of Cu_2O.

	Cu^{2+} (CuO)	Cu^{1+} (Cu_2O)
Bader Charge / |e|	0.974	0.541

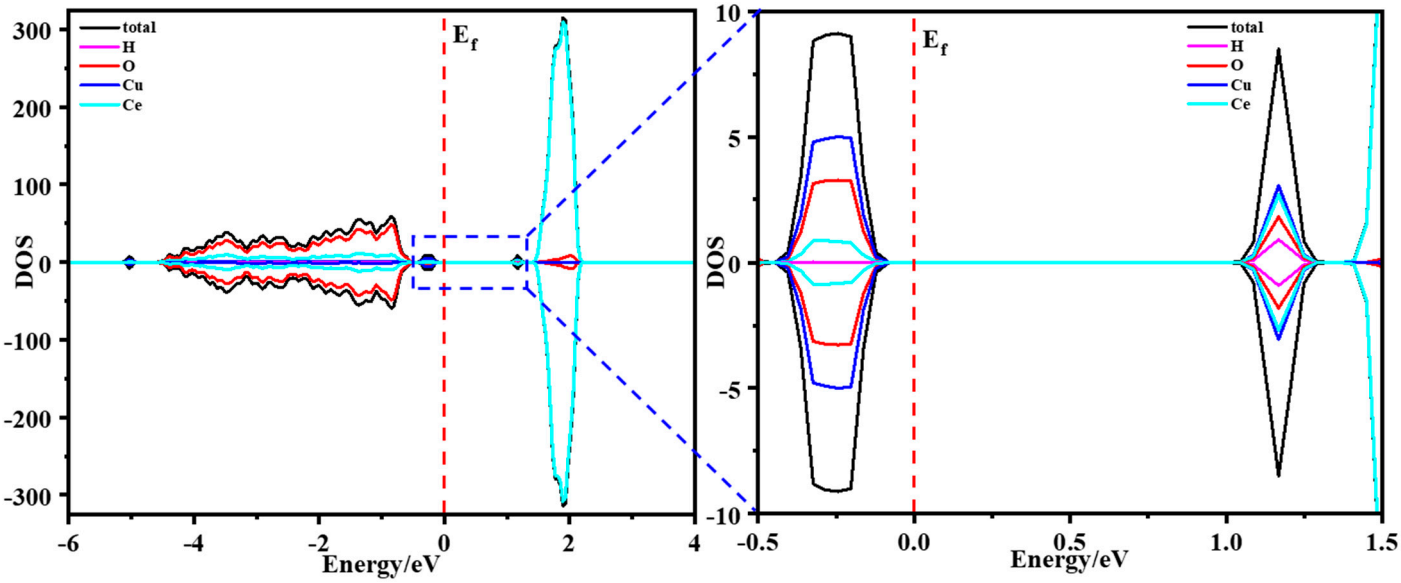

Figure S1. Calculated density of states (DOS) of the Cu/CeO_2(111) surface with H being adsorbed at the Cu site.

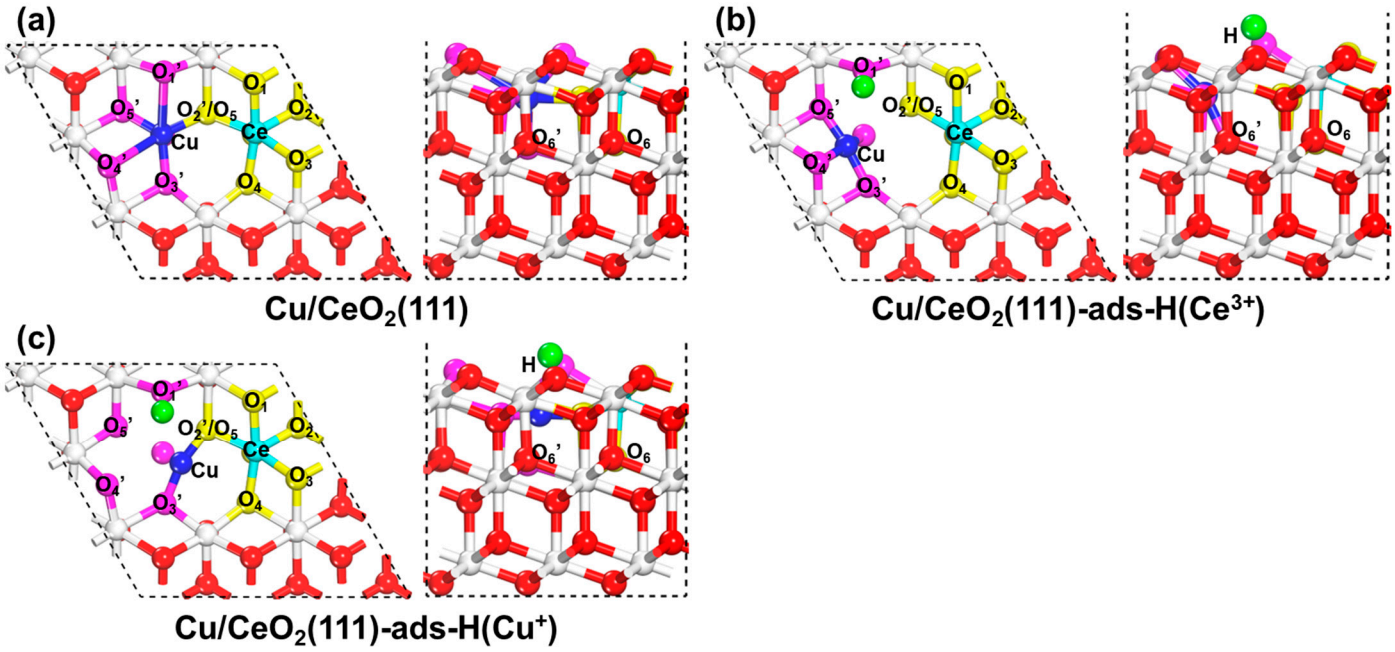

Figure S2. Calculated structures (left: side view; right: top view) of (**a**) Cu/CeO_2(111); calculated structures of Cu/CeO_2(111) with H being adsorbed at the O site and the electron is localized at (**b**) the Ce site and (**c**) the Cu site. Red: O atoms; white and aquamarine: Ce atoms; blue: Cu atoms; green: H atoms; yellow: neighboring oxygen atoms of the Ce; pink: neighboring oxygen atoms of the Cu.

Table S4. Calculated Bader charges of the Cu and Ce species and their nearby O; calculated Cu-O and Ce-O bond distances, and the electrostatic interaction energies (E_{Cu+Ce}) between the Cu and Ce and their nearby species on the Cu/CeO_2(111) and the Cu/CeO_2(111) surface with H being adsorbed at the O site; calculated Cu coordinate numbers on the Cu/CeO_2(111) and the Cu/CeO_2(111) surface with H being adsorbed at the O site (the corresponding structures are illustrated in Figure S2).

	Ce / |e|	**O_1 / |e|**	**O_2 / |e|**	**O_3 / |e|**	**O_4 / |e|**	**O_5 / |e|**	**O_6 / |e|**
Cu/CeO_2(111)	2.351	-1.196	-1.194	-1.196	-1.229	-1.191	-1.227
Ads-H(Ce^{3+})	2.071	-1.220	-1.236	-1.220	-1.255	-1.200	-1.210
Ads-H(Cu^{1+})	2.311	-1.200	-1.196	-1.184	-1.230	-1.182	-1.220
	Cu / |e|	**O_1' / |e|**	**O_2' / |e|**	**O_3' / |e|**	**O_4' / |e|**	**O_5' / |e|**	**O_6' / |e|**
Cu/CeO_2(111)	1.044	-1.102	-1.191	-1.193	-1.104	-1.131	-1.130
Ads-H(Ce^{3+})	0.998	-1.285	-1.200	-1.153	-1.109	-1.122	-1.143
Ads-H(Cu^{1+})	0.656	-1.093	-1.182	-1.173	-1.105	-1.141	-1.173
	Ce-O_1 / Å	**Ce-O_2 / Å**	**Ce-O_3 / Å**	**Ce-O_4 / Å**	**Ce-O_5 / Å**	**Ce-O_6 / Å**	**E_{Cu+Ce} / eV**
Cu/CeO_2(111)	2.279	2.231	2.344	2.318	2.297	2.316	-151.39
Ads-H(Ce^{3+})	2.456	2.300	2.505	2.430	2.392	2.412	-134.05
Ads-H(Cu^{1+})	2.289	2.241	2.315	2.337	2.296	2.318	-130.40
	Cu-O_1' / Å	**Cu-O_2' / Å**	**Cu-O_3' / Å**	**Cu-O_4' / Å**	**Cu-O_5' / Å**	**Cu-O_6' / Å**	**Cu Coordinate Number**
Cu/CeO_2(111)	3.133	2.151	2.148	3.133	1.956	1.909	4
Ads-H(Ce^{3+})	3.825	3.250	1.934	1.970	1.932	1.985	4
Ads-H(Cu^{1+})	3.648	1.868	1.868	3.753	3.216	2.133	3

As it has been explained in the previous work [27,38], the electrostatic interaction energy between the Cu and Ce species and its nearby species, E_{Cu+Ce}, on the Cu/CeO_2(111) and the Cu/CeO_2(111) surface with H being adsorbed at the O site can be calculated as:

$$E_{Cu+Ce} = \sum_{i=1}^{N} \frac{q_{Ce} * q_O}{4 * \pi * \varepsilon_0 * d_{Ce-O}} + \sum_{i=1}^{N} \frac{q_{Cu} * q_O}{4 * \pi * \varepsilon_0 * d_{Cu-O}} \quad \text{(S1)}$$

where q is the calculated Bader charge, d is the bond distance (between Cu or Ce and nearby oxygen species), and ε_0 is the vacuum permittivity (i.e., $8.854187817 \times 10^{-12}$ F/m).

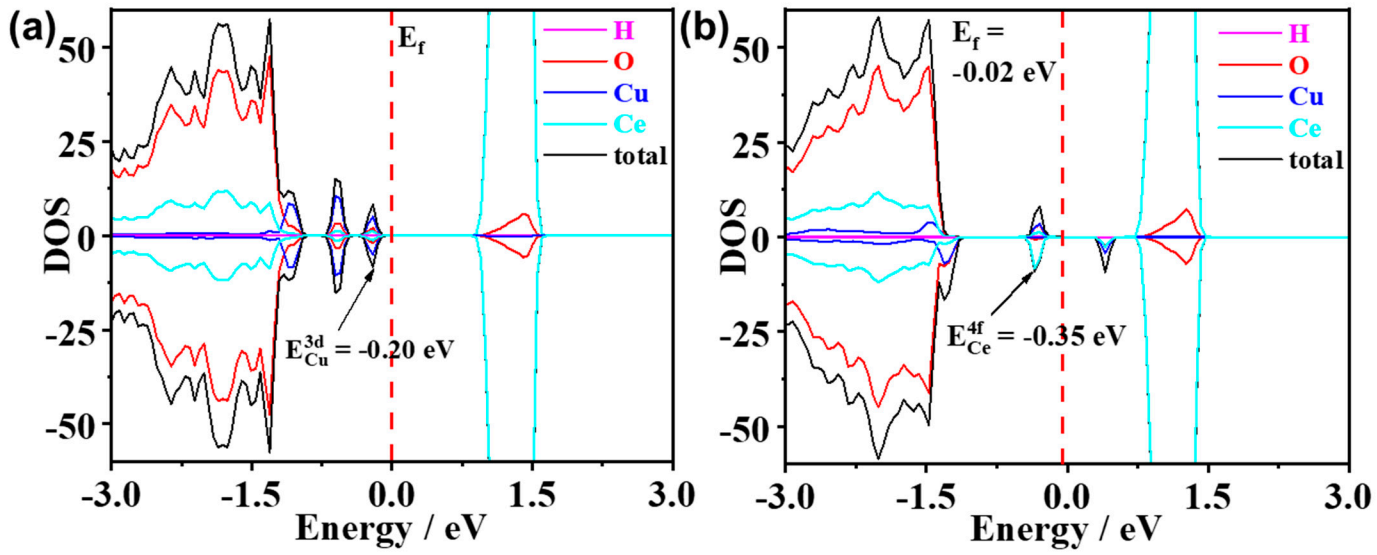

Figure S3. Calculated density of states (DOS) of the Cu/CeO_2(111) surface with H being adsorbed at the O site, (**a**) the electron is localized at the Cu site and (**b**) the electron is localized at the Ce site. All DOS are aligned with respect to the non-interacting O 2*s* orbital of a fixed bottom O atom of surface slabs.

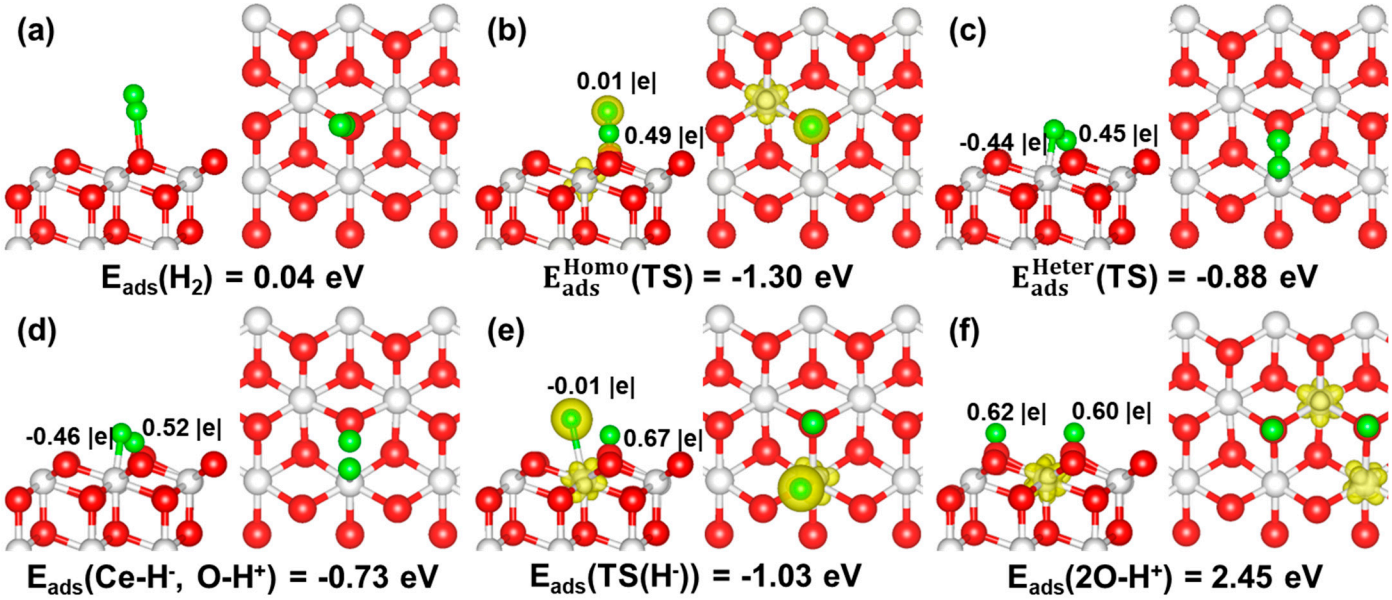

Figure S4. Calculated structures of H_2 adsorption and dissociation on the CeO_2(111) surface. (**a**) H_2 adsorption, (**b**) transition state for H_2 homolytic dissociation, (**c**) transition state for H_2 heterolytic dissociation, (**d**) co-adsorption of H^+ and H^-, (**e**) transition state for the hydride migration to the adjacent oxygen site, (**f**) co-adsorption of two surface H^+ on the oxygen sites. The corresponding adsorption energies and the Bader charges of the H species are also shown.

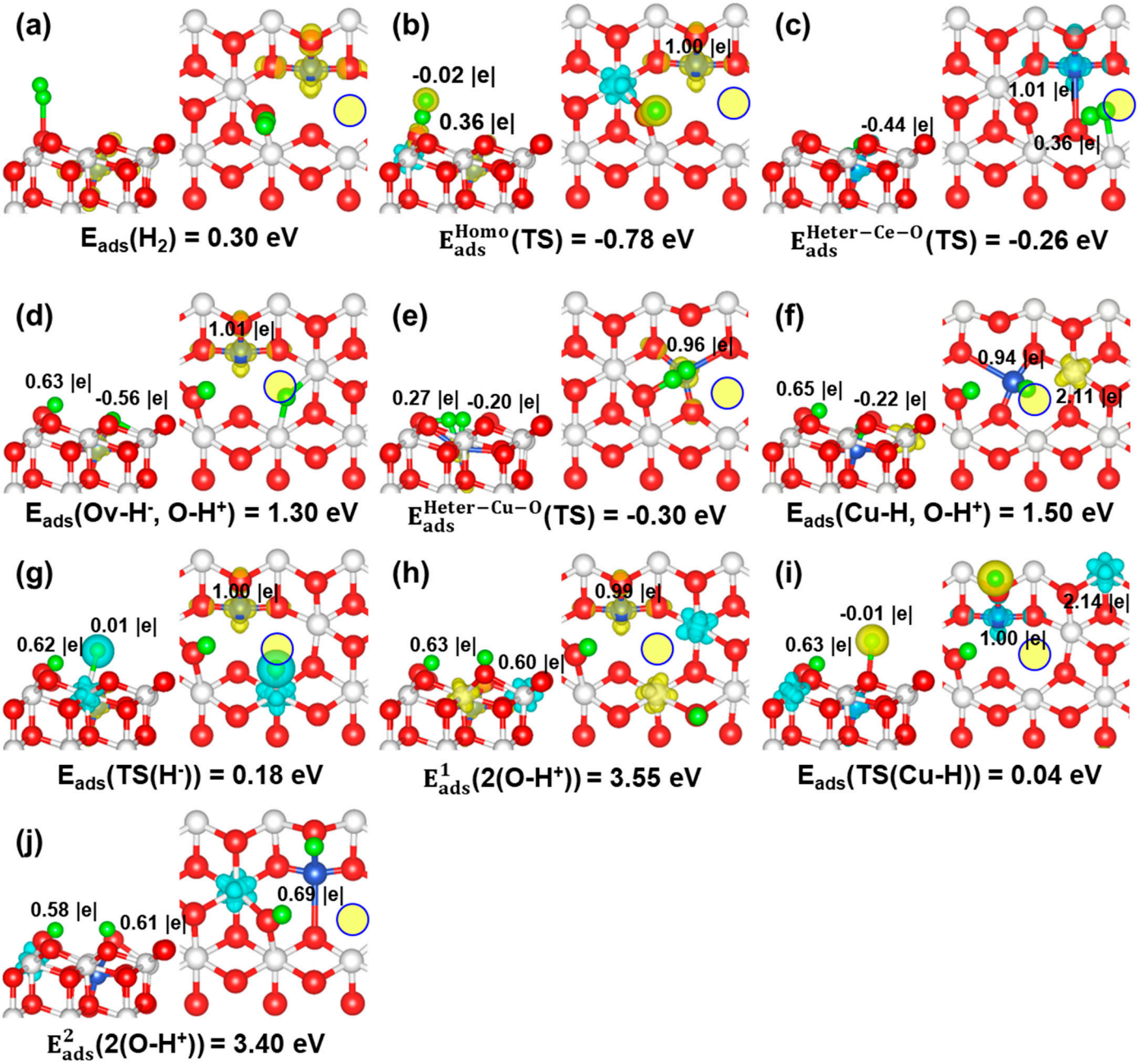

Figure S5. Calculated structures of H_2 adsorption and dissociation on the Cu/CeO_2(111) surface. (**a**) H_2 adsorption, (**b**) transition state for H_2 homolytic dissociation, (**c**) transition state for H_2 heterolytic dissociation above the Ce-O bond, (**d**) co-adsorption of H^+ and H^-, (**e**) transition state for H_2 heterolytic dissociation above the Cu-O bond, (**f**) co-adsorption of H^+ and Cu-H, (**g**) transition state for the hydride migration to the adjacent O_{2c} site, (**h**) co-adsorption of two surface H^+ on two O_{2c} sites, (**i**) transition state for the (Cu-)H migration to the adjacent O_{3c} site, (**j**) co-adsorption of two surface H^+ on the O_{2c} and O_{3c} sites. The corresponding adsorption energies and the Bader charges of the H, Cu and Ce species are also shown.

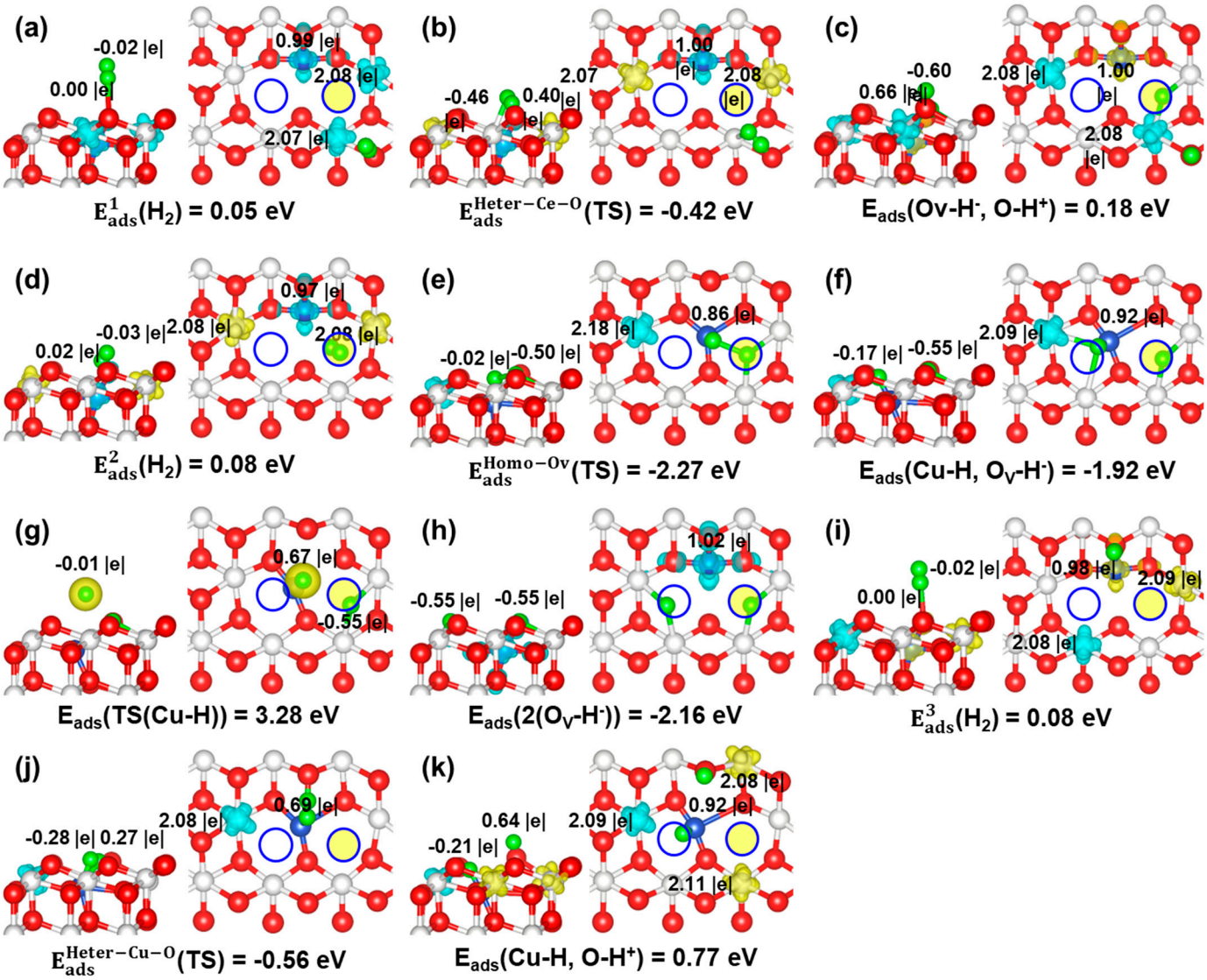

Figure S6. Calculated structures of H_2 adsorption and dissociation on the Cu/CeO_2(111)-O_V surface. (**a**) H_2 adsorption on the oxygen site, (**b**) transition state for H_2 heterolytic dissociation above the Ce-O bond, (**c**) co-adsorption of H^+ and H^-, (**d**) H_2 adsorption on the O_V site, (**e**) transition state for H_2 homolytic dissociation, (**f**) co-adsorption of H^- and (Cu-)H, (**g**) transition state for the (Cu-)H migration to the adjacent O_V site, (**h**) co-adsorption of two H^- on two O_V sites, (**i**) H_2 adsorption above the Cu-O bond, (**j**) transition state for H_2 heterolytic dissociation above the Cu-O bond, (**k**) co-adsorption of H^+ and (Cu-)H. The corresponding adsorption energies and the Bader charges of the H, Cu and Ce species are also shown.

Crystal Reduction Potential (V_r) [57].

In the same spirit as V_r extends useful concepts from atomic/molecular (electro)chemistry, such as ionization energies (E_i) and standard reduction potentials ($V°$), to the solid state by consistently including crystal field effects and removing any solvation effects in an aqueous (or other liquid) medium, we defined the reduction potential (V_r) for $M^{n+} \rightarrow M^{m+}$ (where n > m) as:

$$V_r[M^{n+} \rightarrow M^{m+}] = -E_r[M^{n+} \rightarrow M^{m+}] / (n - m)F \quad (S2)$$

where n and m are the oxidation states of the metals in the ground-state polymorphs of metal-oxide crystals $MO_{n/2}$ and $MO_{m/2}$, respectively, F is the Faraday constant, and $E_r[M^{n+} \rightarrow M^{m+}]$ can be calculated as follows:

$$E_r[M^{n+} \rightarrow M^{m+}] = E^{SCAN+U}[MO_{m/2}] + (n - m)E^{SCAN}[O_2]/4 - E^{SCAN+U}[MO_{n/2}] \quad (S3)$$

Note that V_r in eq 2 is strictly defined for the Gibbs energy (G) of reduction. Here we ignored the PV and entropic effects, and G can be approximated as the DFT energy (*i.e.*, G ≈ E). Then, the calculated V_r value are: $V_r[Ce^{4+} \rightarrow Ce^{3+}]$ = −1.77 V and $V_r[Cu^{2+} \rightarrow Cu^{+}]$ = −1.43 V.

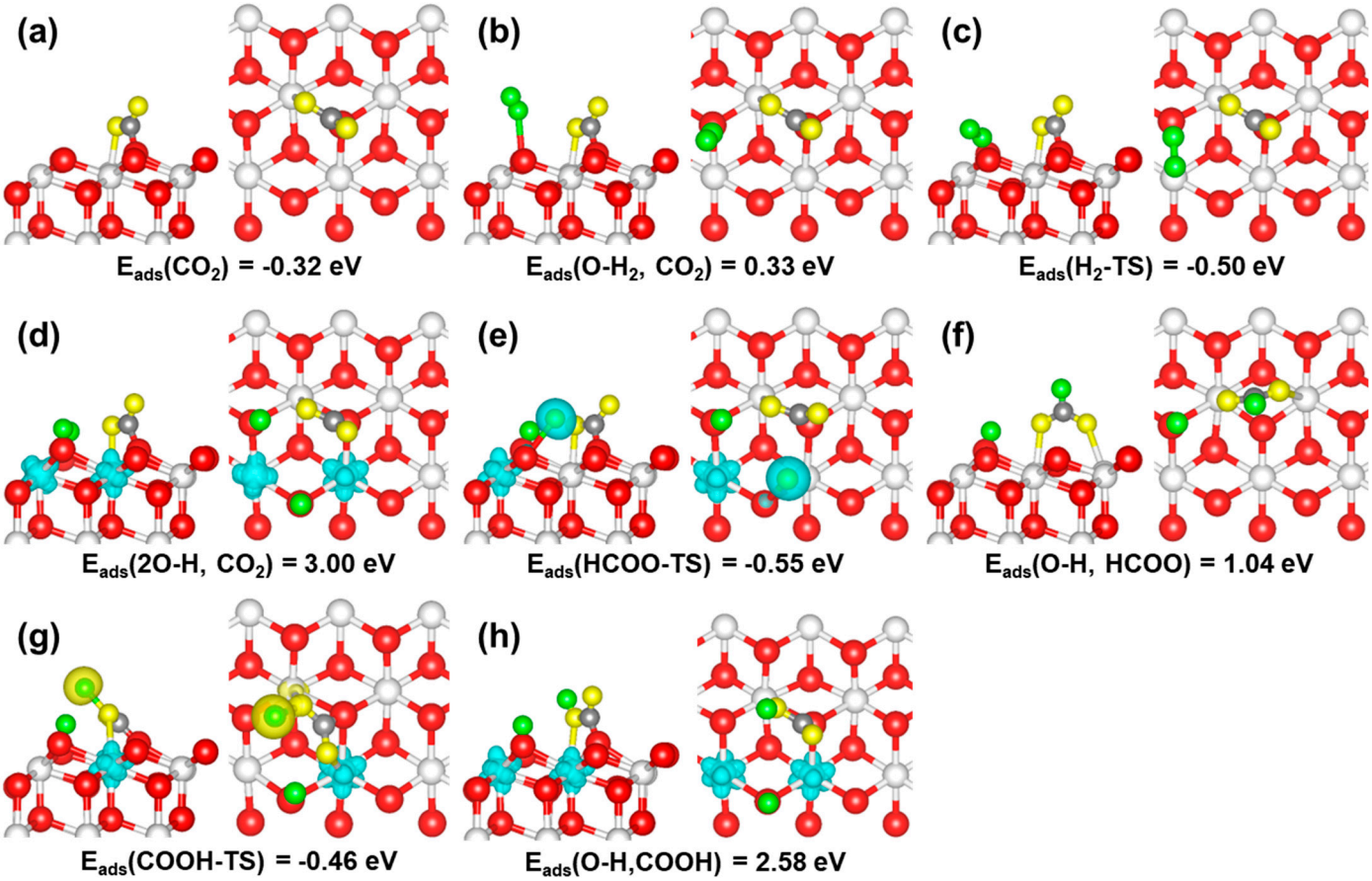

Figure S7. Calculated structures of the (**a**) CO_2 adsorption, (**b**) CO_2 and H_2 co-adsorption, (**c**) transition state for H_2 dissociation, (**d**) dissociated H_2, (**e**) transition state of CO_2 hydrogenation to HCOO, (**f**) co-adsorbed (O-)H and HCOO, (**g**) transition state of CO_2 hydrogenation to COOH, (**h**) co-adsorbed (O-)H and COOH on the CeO_2(111) surface. The corresponding adsorption energies and the spin density distributions are also shown.

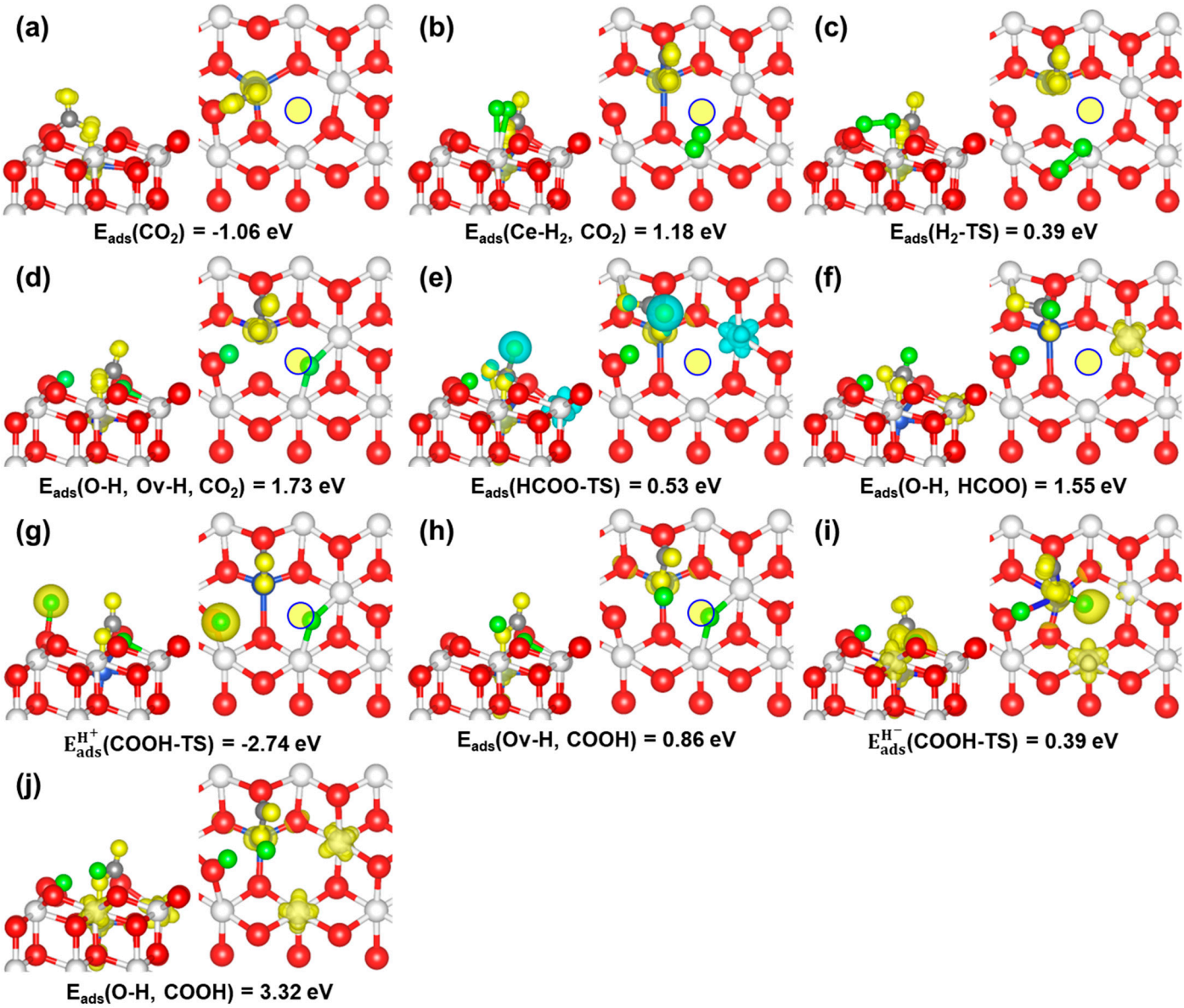

Figure S8. Calculated structures of the (**a**) CO_2 adsorption, (**b**) CO_2 and H_2 co-adsorption, (**c**) transition state for H_2 dissociation, (**d**) dissociated H_2, (**e**) transition state of CO_2 hydrogenation to HCOO, (**f**) co-adsorbed (O-)H and HCOO, (**g**) transition state of CO_2 hydrogenation (by H^+) to COOH, (**h**) co-adsorbed (O_V-)H and COOH, (**i**) transition state of CO_2 hydrogenation (by H^-) to COOH, (**j**) co-adsorbed (O-)H and COOH on the Cu/CeO_2(111) surface. The corresponding adsorption energies and the spin density distributions are also shown.